Published in final edited form as:
J Immunol. 2011 July 1; 187(1): 190–199. doi:10.4049/jimmunol.1004129.

Membrane-bound IL-22 after *de novo* production in tuberculosis and anti-*M.tuberculosis* effector function of IL-22+CD4+ T cells

Gucheng Zeng[1,2,#], **Crystal Y. Chen**[1,#], **Dan Huang**[1,#], **Shuyu Yao**[1], **Richard C. Wang**[1], and **Zheng W. Chen**[1,*]

[1]Department of Microbiology and Immunology, Center for Primate Biomedical Research, University of Illinois College of Medicine, Chicago, IL 60612

Abstract

The role of IL-22-producing CD4+ T cells in intracellular pathogen infections is poorly characterized. IL-22-producing CD4+ T cells may also express other effector molecules, and therefore synergize or contribute to anti-microbial effector function. This hypothesis cannot be tested by conventional approaches manipulating a single IL-22 cytokine at genetic and protein levels, and IL-22+ T cells cannot be purified for evaluation due to secretion nature of cytokines. Here, we surprisingly found that upon activation, CD4+ T cells in *M. tuberculosis*-infected macaques or humans could evolve into T effector cells bearing membrane-bound IL-22 after *de novo* IL-22 production. Membrane-bound IL-22+ CD4+ T effector cells appeared to mature *in vivo* and sustain membrane distribution in highly-inflammatory environments during active *M. tuberculosis* infection. NSOM/QD-based nanoscale molecular imaging revealed that membrane-bound IL-22, like CD3, distributed in membrane and engaged as ~100–200 nm nanoclusters or ~300–600 nm nanodomains for potential interaction with IL-22 receptor. Importantly, purified membrane-bound IL-22+ CD4+ T cells inhibited intracellular *M. tuberculosis* replication in macrophages. Our findings suggest that IL-22-producing T cells can evolve to retain IL-22 on membrane for prolonged IL-22 half-lives and to exert efficient cell-cell interaction for anti-*M. tuberculosis* effector function.

Keywords

Tuberculosis; IL-22; Infection; NSOM/QD; nanoscale molecular imaging

Introduction

Naïve CD4+ T cells can evolve to at least four distinct cell populations, Th1, Th2, Th17 and induced regulatory T cells (iTreg), in response to antigen(1, 2). Th17 cell lineage differentiation is regulated by a master transcription factor, retinoid-related orphan receptor(ROR)γt(1, 2). Murine Th17 cells produce and secret the signature cytokines IL-17, IL-17F and IL-22(1, 2). IL-22 is an IL-10-family cytokine, and is mainly produced by T cells and a subset of natural killer (NK) cells(3–6). Some studies suggest that IL-22 plays a role in development of inflammatory diseases such as rheumatoid arthritis, psoriasis, and inflammatory bowel diseases(7–11). Other studies implicate that IL-22 may protect against

[*]Address correspondence to Dr. Zheng W. Chen, 909 S. Wolcott Ave, MC790, Chicago, IL 60612; Phone, 312 355-0531; Fax, 312 996-6415; zchen@uic.edu.
[2]Current address: Department of Microbiology, Zhongshan School of Medicine, Sun Yat-sen University, Cuangzhou 510080, China
[#]These investigators contributed equally to this work, and should share the first authorship.

Conflict of interests: None

cell injuries (12, 13), and act on IL-22 receptor (IL-22R) to facilitate innate immunity against extracellular bacterial and fungi infections (14–17). It is important to note that immune function of Th17 cells or IL-22+ T cells has been investigated through immune manipulation or targeting of IL-17 or IL-22. Given the possibility that lineage differentiation/maturation and *in vivo* turnover of Th1, Th2, and Th17 cell populations including IL-22+ T effectors are quite plastic and dynamic during infection (1), each of these T effector subsets may represent a heterogeneous cell population producing the IL-17/IL-22 signature cytokine and other effector molecules. From this immunological standpoint, targeting a single IL-17 or IL-22 cytokine in experiments may insufficiently define the function of Th17 T effector cell populations. Use of the IL-17/IL-22 cytokine-expressing Th17 effector cells in experimental investigation may provide additional information regarding the cellular effector function of these cells. However, current biological techniques cannot allow purification or selection of the IL-17/IL-22-producing T-effector cell population due to the secretive nature of cytokines including IL-17/IL-22.

Tuberculosis (TB) remains one of leading causes for morbidity and mortality worldwide among infectious diseases, with annual 8 million new cases and 2 million deaths(18). Although CD4+ T cells and Th1 cytokines are protective against *M. tuberculosis* infection, full anti-TB immunity appears to involve other undefined immune components(19). Understanding roles of other T-cell subsets producing a signature cytokine and other effector molecules should help to elucidate anti-TB immunity and facilitate development of new vaccine and immunotherapeutics against TB. We have recently found that macaque IL-22 transcripts are remarkably increased in lung and lymphoid tissues in severe TB(20), a finding similarly seen in a human study(21). We also demonstrated that while most T effector cells secreting conventional cytokines often cannot be directly detected without *in vitro* Ag re-stimulation, IL-22 protein produced by macaque T cells could be visualized *in situ* even in lung tissues containing TB granuloma (22, 23). Moreover, macaque IL-22+ T cells that have matured during *M. tuberculosis* infection can readily be detected in blood and tissue lymphocytes by intracellular cytokine staining without *in vitro* Ag re-stimulation (23). However, immune function of IL-22-producing CD4+ T cells in *M. tuberculosis* infection remains unknown.

Our finding that IL-22+ T effector cells can be readily detected *in situ* in TB allowed us to hypothesize that IL-22+ T effector cells or IL-22 play a role in *M. tuberculosis* infection and that IL-22 intracellular trafficking/secretion may differ somehow from most other T-cell-producing interleukins (24, 25). In testing this hypothesis, we surprisingly found that IL-22 produced by CD4+ T cells could evolve to retain in cell-membrane, and engage as nanoclusters or nanodomains after *de novo* production in *M. tuberculosis* infection. Notably, membrane-bound IL-22+CD4+ T cells were able to inhibit intracellular *M. tuberculosis* replication in macrophages.

Materials and Methods

Animals

Adult rhesus macaques were used in this study. Macaques were naïve prior to *M. tuberculosis* infection on a basis of tuberculin skin test, IFN-γ ELISOPOT assays, and thoracic radiographs. *M. tuberculosis* infected macaques were housed at the Biologic Research Resources Annex BSL3 nonhuman primate facilities in University of Illinois at Chicago (UIC) and sacrificed after two months of infection. All animal experimental procedures and protocols were approved by the UIC Animal Care Committee.

M. tuberculosis infection of macaques

Each monkey was infected with 500 CFU of *M. tuberculosis* Erdman (the standard challenge stock from FDA) by the bronchoscope-guided injection of the inoculum into the right caudal lobe as previously described (23, 26). This was done in the procedure room at the Annex BSL3 nonhuman primate facilities at UIC. The inoculum used for infection was diluted and plated on 7H11 agar plates (BD) to further confirm the bacterial CFU dose for inoculation.

Isolation of lymphocytes from blood, lung and spleen

PBMC were isolated from freshly collected EDTA blood of macaques or humans by Ficoll-Paque plus (Amersham, Piscataway, NJ) density gradient centrifugation, as described previously(27). For isolation of lymphocytes from lung and spleen tissues, lung and spleen tissues were minced with sharp scissors and squeezed with sterile copper mesh in Petri dish and collected with RPMI followed by filtering through 40-um cell strainers. Mesenteric lymph nodes were carefully teased apart with 18-gauge needle in Petri dish with RPMI to form single cell suspension. Collected cell suspensions from lung, spleen and mesenteric lymph nodes were further purified by Ficoll-Paque plus density gradient centrifugation to collect pure lymphocytes. The freshly isolated lymphocytes from blood, lung, spleen and mesenteric lymph nodes were stained by trypan blue to examine the viability and numerate cell counts. The lymphocytes were finally suspended into 10% FCS-RBMI media with a concentration of 10^7 cells/ml for further study.

Flow cytometry analysis of macaque or human CD4 T cell precursors producing membrane-bound IL-22 and of IL-22 receptor-expressing macrophages

PBMC that isolated freshly from the blood of *M. tuberculosis*-infected macaques or purified protein derivative$(PPD)^+$ or PPD^- human donors were infected with *M. tuberculosis* in 96-well plates in multiplicity of infection (MOI)=1 for 18 hours. And then cells were washed with 2% FBS/PBS and stained without treatment with membrane permeabilization reagents with FITC-CD4 (L200, BD), PE/Cy7-CD3 (SP34-2, BD), IL22-biotinylated or PB (goat anti-human, R&D), and PE-IFN-γ (4S.B3, BD) antibodies for 30 minutes. After washing, cells were incubated with streptavidin-PB (Invitrogen), followed by washing with 2% FBS/PBS. These cells were then fixed with 2% formalin/PBS and analyzed by flow cytometry. IL-22 receptor(IL-22R) expression in macrophages were analyzed by flow-cytometry using APC-IL-22R (305405, R&D system).

Flow cytometry analysis of membrane-bound IL-22 produced by lymphocytes that isolated from the spleens or lungs of *M. tuberculosis*-infected macaques with additional *in vitro* Ag re-stimulation

Cells that isolated freshly from the spleens or lungs of monkeys after two-month infection were stimulated with 15mer overlapping peptides spanning Ag85B and ESAT6 (GenScript) and anti-CD28 (CD28.2, BD) and anti CD49d (9F10, BD) for one hour. After thoroughly washing, these cells were used for antibody staining without treatment with membrane permeabilization reagents. Cells were incubated with FITC-CD4 (L200, BD), PE/Cy7-CD3 (SP34-2, BD), and IL22-biotinylated or -PB (goat anti-human, R&D) antibodies for 30 minutes. After thoroughly washing, cells were incubated with streptavidin-PB (Invitrogen). These cells were then washed twice with 2% FBS/PBS and fixed with 2% formalin/PBS and then analyzed by flow cytometry. To investigate if secretory form of IL-22 also existed, IL-22 in culture supernatants from activated, enriched CD4+ lymphocytes or IL-22+CD4+ T cells was examined using the dot-blot assay as we described(28, 29). We used the dot blot assay as ELISA assay for quantitation of macaque IL-22 was not commercially available. Typically, ~1×10^7 enriched CD4+ T cells from spleens of infected macaques were

stimulated by PPD in culture for two or four days. Supernatants were collected, either un-concentrated or concentrated 50× using Vivacell concentrator (Vivasciences) as we described (28, 29), and then tested for IL-22 by the dot plot assay (28, 29) using the same anti-IL-22 Ab as described above. Negative control was culture supernatants from un-stimulated PBL of uninfected macaques. The specificity of IL-22 antibody staining was confirmed repeatedly using matched normal serum, control antibodies or control animals. No or very few IL-22-producing CD4 T cells were detectable in the longitudinal control experiments (data not shown). Fixed lymphocytes were run on a CyAn ADP flow cytometer (DakoCytomation, Carpinteria, CA) for analysis.

Flow cytometry analysis of membrane-bound IL-22 produced by lymphocytes that isolated from the spleens or lungs of *M. tuberculosis*-infected macaques without additional *in vitro* Ag re-stimulation

Cells that isolated freshly from the spleens or lungs of monkeys after two-month infection were stained directly with antibodies without additional in vitro treatment of antigen or antibodies or membrane permeabilization reagents. Cells were then incubated with FITC-CD4 (L200, BD), PE/Cy7-CD3 (SP34-2, BD), and IL22-biotinylated (goat anti-human, R&D) antibodies for 30 minutes. After thoroughly washing, cells were incubated with streptavidin-PB (Invitrogen). These cells then were washed twice with 2% FBS/PBS and fixed with 2% formalin/PBS and analyzed by flow cytometry.

Experimental controls for assessing membrane-bound IL-22+CD4+ T cells

We found that macaque and human IL-2 shared >98% similarity in amino acid sequence(data not shown), and that the anti-human IL-22 Ab could readily cross-react with soluble macaque IL-22 produced either by *L. lactis* (30) or *Listeria monocytogenes* expression system on dot blot or western blot assay(data not shown). Consistently, non-conjugated anti-human IL-22 Ab pre-treatment of IL-22+ T cells could block the immune staining of membrane-bound IL-22+T cells by fluorescence IL22-biotinylated Ab(see above). In addition, matched normal serum or isotype IgG served as negative controls for staining cytokines or surface markers. We did not see non-specific immune staining of IL-22 as evaluated by flow cytometry, confocal imaging or NSOM/QD-based molecular imaging(see below). Furthermore, to ensure the specific immune staining of membrane-bound IL-22 in *M. tuberculosis* infection, PBMC were obtained biweekly for 8 weeks from three healthy uninfected and five SHIV-infected cynomolgus macaques, and assessed for IL-22-producing T cells using the immune staining assay as described above. No or very few membrane-bound IL-22+CD4+ T cells (<0.02% of CD3) were detectable in the longitudinal control experiments (data not shown).

NSOM/QD-based nanoscale analysis of membrane-bound IL-22 produced by spleen lymphocytes that isolated from *M. tuberculosis*-infected macaques

Cells that isolated from the spleens of monkeys after 8 weeks' infection of *M. tuberculosis* were fixed with 2% formalin/PBS firstly. Our previous works have shown that short-term 2% formalin/PBS would greatly reduce unspecific activation during antibody staining but would not induce significant artificial cellular nanostructures(31–33). These cells then were washed extensively with 2% FBS/PBS and ready for antibody staining. Cells were incubated with mouse anti-human CD4 (L200, BD) and goat anti-human IL-22-biotinylated (R&D) Ab for 30 minutes. After washing with 2% FBS/PBS, these cells were stained with streptavidin-QD655 (Invitrogen) and QD605-goat-anti-mouse IgG (Invitrogen). After incubating with all the antibodies or fluorochromes, cells were fixed with 2% formalin/PBS and washed thoroughly again using 2% FBS/PBS. Cells then were washed again with dd water twice to remove the salt in the PBS. NSOM (Veeco, Aurora 3.0) imaging was done as described in our previous work(30).

Confocal microscopic analysis of membrane-bound IL-22 produced by spleen lymphocytes of *M. tuberculosis*-infected macaques

Cells that isolated from the spleens of monkeys after 8 weeks' infection of *M. tuberculosis* were washed extensively with 2% FBS/PBS and incubated with mouse anti-human FITC-CD4 (L200, BD) and goat anti-human IL-22-biotinylated (R&D) Ab for 30 minutes. After washing with 2% FBS/PBS, these cells were stained with streptavidin-QD655 (Invitrogen). After incubating with all the antibodies or fluorochromes, cells were fixed with 2% formalin/PBS and washed thoroughly again using 2% FBS/PBS. Cells then were washed again with dd water twice to remove the salt in the PBS. Confocal microscopic imaging was done as described in our previous work(30).

In situ confocal microscopic analysis of IL-22 in lung tissue sections of *M. tuberculosis*-infected macaques

≈5-μm-thick frozen lung sections were prepared, as we recently described (34), from optimal cutting temperature compound (OCT)-embedded lung tissues from healthy macaques or *M. tuberculosis*-infected macaques. Tissue sections were first incubated overnight in a wet box with polyclonal rabbit anti-human IL-22 (N-terminus, Capralogics,) and monoclonal mouse anti-human CD3 (F7.2.38, Dako) or isotype control IgG or normal rabbit serum. After thoroughly washed with PBS, tissue sections were fixed with 2% formalin/PBS and washed thoroughly with PBS. Tissue sections were then incubated with FITC-conjugated donkey anti-rabbit IgG (Biolegend) and Cy3-conjugated goat anti-mouse IgG (Biolegend, USA), followed by thorough PBS washing. Next, tissue sections were fixed gently with 2% formalin/PBS again and washed thoroughly with dd water to remove the salt in PBS. Finally, tissue sections were mounted on slides using fluorescence mounting medium with 4', 6-diamidino-2-phenylindole (DAPI) for confocal microscope (Zeiss, LSM 510, (63×NA) imaging.

In situ NSOM/QD-based nanoscale analysis of IL-22 in lung tissue sections of *M. tuberculosis*-infected macaques

The tissue preparation and the primary antibody staining are the same for the confocal microscopic imaging. After primary antibody staining, tissue sections were washed and incubated with QD655-conjugated goat-anti-mouse secondary antibody and QD605-conjugated-goat-anti-rabbit secondary antibody. These tissue sections were then washed thoroughly and fixed with 2% formalin/PBS again and washed thoroughly with dd water to remove the salt in PBS. Then, these tissue sections were imaged with dual-color NSOM/QD-based nanoscale imaging system (Veeco, Aurora3.0).

Isolation of monocytes and membrane-bound IL-22+ CD4+ T cells

PBMC were isolated from the blood of *M. tuberculosis*-infected macaques, and monocytes were obtained by adherence purification on plastic plates (Falcon company), as described previously(27). The plates were washed after 2 h of adherence, and monocytes were detached by cold 2%FBS/PBS. The non-adherent cell fraction containing T cells and B cells was stimulated with PPD in the presence of anti-CD3/anti-CD28 antibodies (BD company) to generate large numbers of membrane-bound IL-22+CD4+ T cells. After overnight culture, the stimulated T-cells were stained with by anti-IL-22-PE (R&D), followed by anti-PE magnetic beads (Miltenyi Biotec). The stained live cells were then loaded to the purification column following instructions from the manufacturer. The passing fraction was collected as IL-22-(negative) cells that did not bear membrane-bound IL-22; IL-22+ T cells held by anti-PE magnetic beads were then released by releasing buffer (Miltenyi Biotec). The isolated IL-22+ T cells were stained again with anti-CD4-FITC (BD), followed by anti-FITC magnetic microbeads for secondary purification.

In vitro M. tuberculosis infection of monocyte-derived macrophages or immature DCs and intracellular *M. tuberculosis* growth assay

Autologous monocytes (5×10^4/well) were cultured in round-bottom 96-well plates with 10% FBS-RPMI1640 medium in the presence of recombinant hIL-4 (BD) and GM-CSF (Sigma) for 4 days as previously described (35). Supernatants were then removed and *M. tuberculosis* inoculums was added at a MOI =1. After 3 h of incubation at 37°C, supernatants were aspirated and each well was washed three times to remove non-ingested mycobacteria. Enriched IL-22+ CD4+ T cells (5×10^5) were incubated with anti-IL-22 neutralizing Ab (10 μg/ml, 142928, R&D) or mouse IgG (10 μg/ml) and cultured in the presence of each of them, as indicated in the section of results. Autologous, bead-enriched $CD20^+$ B cells, $CD25^-CD4^+$ T cells, or $IL\text{-}22^-CD4^+$ T cells (5×10^5 for each subset) served as a control. For the non-contact setting in Transwell culture system (Corning) experiments, enriched IL-22+ CD4+ T cells (5×10^5) were placed in the upper chamber of Transwell culture system without “physical” contact with Mtb-infected macrophages(5×10^4) that were cultured in the lower chamber. Therefore, non-contact IL-22+CD4+ T cells were not able to contact macrophages but secretory IL-22 could trans-pass through the micro-holes and reach macrophages in the lower chamber. Secretory IL-22 was detectable in the concentrated culture medium. For the contact setting, enriched IL-22+CD4+ T cells and infected macrophages were co-cultured in the lower chamber of Transwell culture system. After culturing in 5% CO_2 at 37°C for 4 days, wells were aspirated, and 100 μl of lysis buffer (0.067% SDS in Middlebrook 7H9) was added to each well. Plates were incubated at 37°C for 10 min followed by neutralization of SDS with 300 μl of PBS with 20% BSA. Lysates from each well were pooled, and two 10-fold serial dilutions of lysate in 7H9 medium were made. Aliquots of each dilution of lysate and supernatant were plated onto Middlebrook 7H10 agar and incubated for 3 weeks in 5% CO_2 at 37°C until colonies were large enough to be counted. GM-CSF/hIL-4 treatment alone only induced background level of IL-22R expression, but subsequent *M. tuberculosis* infection of macrophages or immature DC induce apparent IL-22R expression (data not shown).

Statistical analysis

Statistical analysis was done using Student’s *t*-test as previously described(30). $p<0.05$ was considered statistically significant.

Results

Upon activation, CD4+ T cells in *M. tuberculosis*-infected macaques and humans differentiated into T effector cells bearing membrane-bound IL-22 after *de novo* IL-22 production

Although IL-22, like most other cytokines, should be secretory (21, 36), cell membrane-bound IL-22 after *de novo* production may enjoy longer half-life and exert better effector effects on IL-22R+ target cells via surface-molecule interactions between a IL-22+ T cell and a IL-22R+ cell. The notion for membrane-bound IL-22 appears consistent with our recent observation indicating that IL-22+ T cells matured during *M. tuberculosis* infection could directly be detected *in situ* even in lung tissues or directly by intracellular IL-22 staining(22, 23). We therefore hypothesized that TB-induced IL-22+ T cells could have their IL-22 to retain in cell membrane after *de novo* production, and thus readily be detected by surface immune staining. To test this hypothesis, PBMC from *M. tuberculosis*-infected macaques were cultured with *M. tuberculosis* for activation, and assessed for cell-membrane-bound IL-22+ T effector cells after *de novo* IL-22 production using cell surface cytokine staining which skipped the treatment with cell-membrane permeabilization reagents. Interestingly, significant numbers of CD4+ T effector cells bearing membrane-bound IL-22 were detected in PBMC from *M. tuberculosis*-infected macaques but not from

un-infected ones (Fig.1A, 1C). In contrast, very few membrane-bound IFN-γ+ T cells were detectable by direct cell surface staining in PBMC from the same macaques (Fig. 1A, C). Consistently, appreciable numbers of CD4+ T cells bearing membrane-bound IL-22 but not IFN-γ were also detected by direct cell surface staining after *M. tuberculosis* stimulation of PBMC from latently *M. tuberculosis*-infected humans (Fig. 1B, D). We did not observe any co-expression of Th1 cytokines by IL-22+CD4+T cells (Fig.1E). The membrane-bound IL-22 could also be seen by fluorescence membrane imaging (Fig.1F), although secretory form of IL-22 also existed in culture supernatants of activated CD4+ T effectors (Fig.1G). These results therefore suggested that significant numbers of CD4+ T cells in mycobacterium-infected macaques and humans could differentiate into effector cells armed with membrane-bound IL-22 in response to *M. tuberculosis* stimulation *in vitro*.

Membrane-bound IL-22+ CD4+ T cells matured *in vivo* and sustained in highly inflammatory environments during active *M. tuberculosis* infection

We then asked a question as to whether membrane-bound IL-22+ T effector cells could mature and sustain *in vivo* under highly inflammatory environments during active *M. tuberculosis* infection. To address this straightforward question, macaques were infected with *M. tuberculosis* by bronchoscope-guided inoculation as previously described (35), and assessed directly for membrane-bound IL-22+ CD4+ T cells using surface immune staining without *in vitro* stimulation and membrane-permibilization. Surprisingly, appreciable percentage numbers (0.82±0.09%) of spleen CD4+ T cells bearing membrane-bound IL-22 could be detected without *in vitro* culture and membrane-permeabilization treatment (Fig. 2A, B). A short-term *in vitro* re-stimulation of spleen lymphocytes by pooled ESAT-6 and Ag85B peptides resulted in the increased percentage numbers (3.03±0.66%) of membrane-bound IL-22+ CD4+ T cells, suggesting that IL-22 binds to and retains in membrane after *de novo* production in newly-generated IL-22+ T effector cells (Fig.2A, B). Consistently, the mature CD4+ T effector cells bearing membrane-bound IL-22 appeared to be driven by bacterial antigen loads *in vivo* since greater percentages (3.91±1.66%) of these effector T cells could be detected directly without Ag re-stimulation in lymphocytes isolated from *M. tuberculosis*-infected lung tissues of the same macaques in comparisons with blood and spleen lymphocytes (Fig.2A, B, and (37). The number of membrane-bound IL-22+ T cells from the lung was only subtly increased after the *in vitro* Ag stimulation (4.67±1.88%) (Fig. 2A, B), suggesting that most of these lung IL-22+ T cells matured enough *in vivo* and sustained their capability to retain IL-22 on membrane without rapid degradation after *de novo* production in highly inflammatory environments during *M. tuberculosis* infection.

Membrane-bound IL-22 molecules distributed in membrane and engaged as ~100–200nm nanoclusters or ~300–600 nm high-density nanodomains on membrane of IL-22+CD4+ T effectors

Studies from us and others suggests that during cellular signaling/activation, cell-membrane ligands or receptors undergo instructed engagements forming clusters or capping domains to enhance ligand-receptor interaction between the two contact cells and to sustain cellular activation (32, 38, 39). Thus, we hypothesized that membrane-bound IL-22 molecules might engage themselves forming unique nanostructures for putative interaction with IL-22R on responsive cells. To test this hypothesis, we employed our expertise of confocal imaging and near-field optical microscopy (NSOM)/quantum dot (QD)-based nanoscale molecular imaging(30, 32, 39) to visualize membrane-bound nature and nanostructures of IL-22 molecules. Confocal microscopy showed that IL-22 on the surface of spleen CD4+ T effectors localized as large capping domains (Fig. 3A), but could not confer high-resolution nanoscale imaging of molecular details. In contrast, our novel NSOM/QD-based nanoscale imaging system, which exclusively images cell-surface membrane molecules but not intracellular contents of intact cells(30, 32, 39), revealed that IL-22 cytokine proteins

engaged themselves as ~100–200 nm nanoclusters on outer membrane (Fig. 3B). Some of these IL-22 nanoclusters were arrayed to form ~300–600 nm nanodomains (Fig.3B and C). The formation of these IL-22 nanoclulsters or nanodomains on membrane suggested that large amounts of IL-22 were retained on T-cell membrane and actively involved in immune responses during active *M. tuberculosis* infection. However, these membrane-bound IL-22 nanoclusters were seldom co-localized with CD4 molecules (Fig.3B, merge).

To examine if IL-22 was distributed within membrane rather than simply attached to the very surface of membrane, we dissected cross-sectional membrane and intracellular compartments of individual IL-22+ T effector cells in lung tissues containing TB granulomas using *in situ* confocal microscopy and NSOM/QD imaging techniques. Confocal images showed that IL-22, but not IFN-γ or IL-4, could be reproducibly detected on CD3+ T cells in the sections derived from lung tissues containing TB granulomas (Fig.4A). Under confocal microscopy, IL-22 and CD3 appeared to exhibit similar membrane distribution in the lung sections (Fig.4A). Consistently, NSOM/QD-based nanoscale imaging showed that IL-22 cytokine proteins were distributed as nanoclusters/nanodomains in membrane rather than in the cytoplasm of effector cells in the lung sections (Fig. 4B, C and D). IL-22 indeed shared distribution patterns with membrane CD3 molecules (Fig.4B). Some IL-22 nanoclusters appeared to co-localize with CD3 nanoclusters (Fig. 4B). Collectively, these results suggest that membrane-bound IL-22 molecules distributed in membrane and engaged as ~100–200 nanoclusters or ~300–600 nm high-density nanodomains on membrane of IL-22+CD4+ T effectors in *M. tuberculosis* infection.

Membrane-bound IL-22+ CD4+ T cells inhibited intracellular *M. tuberculosis* replication in macrophages

The role of IL-22-producing CD4 T effector cells in *M. tuberculosis* infection remains unknown. Now, our identification of CD4+ T effector cells bearing membrane-bound IL-22 made it possible to isolate IL-22+CD4+ T cells and to determine if these cells could have positive or negative impact on intracellular *M. tuberculosis* replication in IL-22R-expressing macrophages or DC (Fig. 5A). Thus, monocyte-derived macrophages or DCs were infected with *M. tuberculosis*, and co-cultured with autologous membrane-bound IL-22+CD4+ T cells that were purified from macaque PBL using immunomagnetic beads, as we described previously(35, 39). This procedure enriched membrane-bound IL-22+CD4+ T cells to the level of 70–96%(Fig.5B). Purified autologous B cells, CD25-CD4+ T cells and IL-22-CD4+ T cells served as controls, respectively. Interestingly, the purified membrane-bound IL-22+ CD4+ T cells significantly inhibited intracellular *M. tuberculosis* replication in cultured macrophages (Fig. 5C). Such inhibition of *M. tuberculosis* replication appeared to be mediated at least in part by membrane-bound IL-22 as anti-IL-22 neutralizing Ab could significantly reverse the inhibition (Fig. 5C) and as the intracellular *M. tuberculosis* growth was inhibited only by membrane IL-22+CD4+ T cells contacting with Mtb-infected macrophages, but not by those non-contacting IL-22+CD4+ T cells or culture medium containing IL-22 secreted by the effector cells((Fig.5D). The *in vitro* work therefore provided novel evidence demonstrating that membrane-bound IL-22+ CD4+ T cells could inhibit intracellular *M. tuberculosis* replication in macrophages.

Discussion

In the current study, we made an unexpected discovery that IL-22-producing CD4+ T cells in *M. tuberculosis*-infected macaques and humans could retain or held IL-22 in cell membrane after *de novo* production. This observation was confirmed by flow cytometry-based surface immune staining, confocal microscopy, and most importantly, NSOM/QD-based nanoscale imaging. The NSOM/QD-based nanoscale imaging on cell surface indeed provides most direct evidence for the membrane-bound IL-22 as NSOM scans and detects

molecules or signals exclusively on the cell surface but not the underneath when cell surface is scanned(32, 39). NSOM/QD imaging of cross-sectional membrane in tissue sections also suggests that membrane IL-22 molecules are distributed in membrane sharing distribution patterns with membrane CD3. IL-22 is therefore one of the very few cytokines with both secretory and membrane-bound forms (24, 25), although conventional protein chemistry and immunology studies suggest that the mature IL-22 protein, like other cytokines, is likely secreted to the extracellular environment(40). Nevertheless, the secretory human or macaque IL-22 proteins appeared to exist as well in TB BAL fluid and culture medium after *in vitro* immune stimulation[(21), Fig.1G]. The precise mechanism whereby IL-22 retains in the membrane is currently not known. Both human and macaque mature IL-22 do not carry classical trans-membrane sequences, and we found no evidence that TB could induce variant IL-22 mRNA encoding additional trans-membrane domains in the C terminal (data not shown). It is important to note that membrane-bound IL-22+ CD4+ T cells can directly be detected without *in vitro* antigen stimulation in spleen cells and lymphocytes from lung tissues containing TB granuloma, suggesting that membrane-bound IL-22 possesses long half lives and sustains even in TB inflammatory environments.

Notably, membrane-bound IL-22 cytokine molecules are engaged as ~100–200nm nanoclusters or ~300–600 nm high-density nanodomains on outer membrane of CD4+ T effector cells that mature *in vivo*. It is also noteworthy that IL-22 nanoclusters or nanodomains co-exist with CD4 and CD3 nanoclusters or nanodomains on membrane of IL-22+ T effector cells. T cells bearing membrane nanoclusters/nanodomains of IL-22, CD4 and CD3 appear to be highly activated effector cells during *M. tuberculosis* infection or in granulomas formation, since we and others shows that occurrence of CD3 and CD4 nanoclusters or nanodomains is a structured engagement of T-cell activation for efficient T-cell receptor interaction with APC and for sustaining T-cell activation (38, 39). More importantly, such membrane IL-22 nanoclusters or nanodomains may confer high-affinity interaction with IL-22R on responsive cells. Thus, membrane-bound IL-22+ CD4+ T cells appear to be immunologically selected to exert prolonged and high-affinity effects on IL-22R-expressing cells in infections.

Our results provided the first evidence that purified IL-22+ CD4+ T cells could mediate inhibition of intracellular *M. tuberculosis* replication in monocyte-derived macrophages. Th1, Th2, Th17 and Treg cells are four major CD4 T helper subsets that can differentiate from naïve CD4+ T cells during infections(1). To date, anti-microbial effector function of human Th17, Th1, and Th2 subsets themselves have remained poorly defined, since it is impossible to isolate or purify each of these T helper subsets for functional analyses. The membrane-bound IL-22 as surface marker allowed us to isolate IL-22+ Th22 cells and evaluate their anti-microbial function. Using this approach, we demonstrated that IL-22+ T cells themselves could inhibit intracellular *M. tuberculosis* in macrophages in the culture system. To our knowledge, this is also the first demonstration that a purified T helper subset is able to directly mediate the inhibition of intracellular bacterium *in vitro* although soluble IL-22 has been shown to limit *M. tuberculosis* growth(41). The membrane IL-22 bioactivity appeared to be supported by the fact that membrane-bound IL-22 in purified T cells could be detected for 2–3 days in cultures(data not shown), and that anti-IL-22 Ab incubation with purified IL-22+CD4+ T cells from the beginning throughout the assay could reduce the effector cells' ability to limit *M. tuberculosis* growth. The result from Transwell system-based experiments also suggests that membrane-bound IL-22 appears to be responsible for the IL-22+CD4+ T effector-mediated restriction of *M. tuberculosis* replication in macrophages as *M. tuberculosis* growth is inhibited by membrane-bound IL-22+ CD4+ T cells contacting with Mtb-infected macrophages, but not by those non-contacting IL-22+CD4+ T cells or culture medium containing soluble IL-22 secreted by the effector cells(Fig.5D). Membrane-bound IL-22 may act on IL-22R expressed in *M. tuberculosis*-

infected macrophages as our new studies demonstrate that while IL-22R is constitutively expressed in epithelial cells, IL-22R expression can also be induced by *M. tuberculosis* infection of macrophages (Fig.5A, and Dan et al, manuscript in preparation). This is also supported by our previous observation that TB induces up-regulation of IL-22R transcript(IL-22Rβ(IL-10Rβ)(20). Thus, our results is consistent with the previous findings that IL-22 can exert anti-microbial activity against extracellular or intracellular pathogens(14–17, 41). The recent human study suggests that soluble IL-22 can limit *M. tuberculosis* growth in macrophages through a mechanism of enhancing phagolysosomal fusion(41). Here, we cannot exclude other cytokines or interacting molecules of the IL-22+CD4+ T cells also contribute to or synergize the *in vitro* anti-*M. tuberculosis* effector function(42). Our previous observations support the hypothesis that IL-22+ T cells may function as either proinflammatory or anti-microbial elements in *M. tuberculosis* infection, depending upon the magnitude of bacterial burdens that elicit optimal or overreacting IL-22+ T effector cells(23). Now the new finding from the current study raises the possibility to define the *in vivo* function of membrane-bound IL-22+ T cells or IL-22 cytokine during *M. tuberculosis* infection of nonhuman primates.

Acknowledgments

We thank Dr. ML Chen for confocal microscopic technical assistance, Jewell Graves, Brenda Paige, and Juan Chen for flow cytometry assistance, Dr. Lisa Halliday for animal work assistance, and PY Teng for NSOM data analysis.

This work was supported by the National Institutes of Health R01 grants: HL64560 (to ZWC), RR13601 (to ZWC). NSOM imaging was supported in part by Sino National Natural Science Foundation grant NNSFC 30828028.

Abbreviations

IL-22	interleukin-22
M. tuberculosis	*Mycobacterium tuberculosis*
TB	Tuberculosis
IL-4	interleukin-4
IFN-γ	Interferon-γ
NSOM	near-field scanning optical microscopy
QD	quantum dot
FWHM	full width at half maximum
Ag	antigen
Ab	antibody
ICS	Intracellular cytokine staining
PPD	Purified Protein Derivative

References

1. Zhou L, Chong MM, Littman DR. Plasticity of CD4+ T cell lineage differentiation. Immunity. 2009; 30:646–655. [PubMed: 19464987]
2. Zhu J, Paul WE. CD4 T cells: fates, functions, and faults. Blood. 2008; 112:1557–1569. [PubMed: 18725574]
3. Luci C, Reynders A, Ivanov II, Cognet C, Chiche L, Chasson L, Hardwigsen J, Anguiano E, Banchereau J, Chaussabel D, et al. Influence of the transcription factor RORgammat on the

development of NKp46+ cell populations in gut and skin. Nat Immunol. 2009; 10:75–82. [PubMed: 19029904]

4. Zenewicz LA, Yancopoulos GD, Valenzuela DM, Murphy AJ, Stevens S, Flavell RA. Innate and adaptive interleukin-22 protects mice from inflammatory bowel disease. Immunity. 2008; 29:947–957. [PubMed: 19100701]
5. Cella M, Fuchs A, Vermi W, Facchetti F, Otero K, Lennerz JK, Doherty JM, Mills JC, Colonna M. A human natural killer cell subset provides an innate source of IL-22 for mucosal immunity. Nature. 2009; 457:722–725. [PubMed: 18978771]
6. Bettelli E, Korn T, Oukka M, Kuchroo VK. Induction and effector functions of T(H)17 cells. Nature. 2008; 453:1051–1057. [PubMed: 18563156]
7. Andoh A, Zhang Z, Inatomi O, Fujino S, Deguchi Y, Araki Y, Tsujikawa T, Kitoh K, Kim-Mitsuyama S, Takayanagi A, et al. Interleukin-22, a member of the IL-10 subfamily, induces inflammatory responses in colonic subepithelial myofibroblasts. Gastroenterology. 2005; 129:969–984. [PubMed: 16143135]
8. Ikeuchi H, Kuroiwa T, Hiramatsu N, Kaneko Y, Hiromura K, Ueki K, Nojima Y. Expression of interleukin-22 in rheumatoid arthritis: potential role as a proinflammatory cytokine. Arthritis Rheum. 2005; 52:1037–1046. [PubMed: 15818686]
9. Zheng Y, Danilenko DM, Valdez P, Kasman I, Eastham-Anderson J, Wu J, Ouyang W. Interleukin-22, a T(H)17 cytokine, mediates IL-23-induced dermal inflammation and acanthosis. Nature. 2007; 445:648–651. [PubMed: 17187052]
10. Ma HL, Liang S, Li J, Napierata L, Brown T, Benoit S, Senices M, Gill D, Dunussi-Joannopoulos K, Collins M, et al. IL-22 is required for Th17 cell-mediated pathology in a mouse model of psoriasis-like skin inflammation. J Clin Invest. 2008; 118:597–607. [PubMed: 18202747]
11. Wilson MS, Feng CG, Barber DL, Yarovinsky F, Cheever AW, Sher A, Grigg M, Collins M, Fouser L, Wynn TA. Redundant and pathogenic roles for IL-22 in mycobacterial, protozoan, and helminth infections. J Immunol. 2010; 184:4378–4390. [PubMed: 20220096]
12. Zenewicz LA, Yancopoulos GD, Valenzuela DM, Murphy AJ, Karow M, Flavell RA. Interleukin-22 but not interleukin-17 provides protection to hepatocytes during acute liver inflammation. Immunity. 2007; 27:647–659. [PubMed: 17919941]
13. Sugimoto K, Ogawa A, Mizoguchi E, Shimomura Y, Andoh A, Bhan AK, Blumberg RS, Xavier RJ, Mizoguchi A. IL-22 ameliorates intestinal inflammation in a mouse model of ulcerative colitis. J Clin Invest. 2008; 118:534–544. [PubMed: 18172556]
14. Wolk K, Kunz S, Witte E, Friedrich M, Asadullah K, Sabat R. IL-22 increases the innate immunity of tissues. Immunity. 2004; 21:241–254. [PubMed: 15308104]
15. Liang SC, Tan XY, Luxenberg DP, Karim R, Dunussi-Joannopoulos K, Collins M, Fouser LA. Interleukin (IL)-22 and IL-17 are coexpressed by Th17 cells and cooperatively enhance expression of antimicrobial peptides. J Exp Med. 2006; 203:2271–2279. [PubMed: 16982811]
16. Zheng Y, Valdez PA, Danilenko DM, Hu Y, Sa SM, Gong Q, Abbas AR, Modrusan Z, Ghilardi N, de Sauvage FJ, et al. Interleukin-22 mediates early host defense against attaching and effacing bacterial pathogens. Nat Med. 2008; 14:282–289. [PubMed: 18264109]
17. Aujla SJ, Chan YR, Zheng M, Fei M, Askew DJ, Pociask DA, Reinhart TA, McAllister F, Edeal J, Gaus K, et al. IL-22 mediates mucosal host defense against Gram-negative bacterial pneumonia. Nat Med. 2008; 14:275–281. [PubMed: 18264110]
18. Wirth T, Hildebrand F, Allix-Beguec C, Wolbeling F, Kubica T, Kremer K, van Soolingen D, Rusch-Gerdes S, Locht C, Brisse S, et al. Origin, spread and demography of the Mycobacterium tuberculosis complex. PLoS Pathog. 2008; 4:e1000160. [PubMed: 18802459]
19. Kaufmann SH. How can immunology contribute to the control of tuberculosis? Nat Rev Immunol. 2001; 1:20–30. [PubMed: 11905811]
20. Qiu L, Huang D, Chen CY, Wang R, Shen L, Shen Y, Hunt R, Estep J, Haynes BF, Jacobs WR Jr, et al. Severe tuberculosis induces unbalanced up-regulation of gene networks and overexpression of IL-22, MIP-1alpha, CCL27, IP-10, CCR4, CCR5, CXCR3, PD1, PDL2, IL-3, IFN-beta, TIM1, and TLR2 but low antigen-specific cellular responses. J Infect Dis. 2008; 198:1514–1519. [PubMed: 18811584]

21. Scriba TJ, Kalsdorf B, Abrahams DA, Isaacs F, Hofmeister J, Black G, Hassan HY, Wilkinson RJ, Walzl G, Gelderbloem SJ, et al. Distinct, specific IL-17- and IL-22-producing CD4+ T cell subsets contribute to the human anti-mycobacterial immune response. J Immunol. 2008; 180:1962–1970. [PubMed: 18209095]
22. Zeng G, Huang D, Chen CY, Shen L, Wang RR, Chen ZW. In situ Visualization of IL-22 Cytokine Response in Tuberculosis, Reply to vani et Al. J Infect Dis. 2009; 200:482–484.
23. Yao S, Zeng G, Huang D, Chen CY, Halliday L, Wang RR, Chen ZW. Differentiation, distribution, and immune regulation of IL-22-producing Th17 cells during *M. tuberculosis* infection of macaques. PLoS Pathog. 2009 in press.
24. Bruns H, Meinken C, Schauenberg P, Harter G, Kern P, Modlin RL, Antoni C, Stenger S. Anti-TNF immunotherapy reduces CD8+ T cell-mediated antimicrobial activity against Mycobacterium tuberculosis in humans. J Clin Invest. 2009; 119:1167–1177. [PubMed: 19381021]
25. Ostroukhova M, Qi Z, Oriss TB, Dixon-McCarthy B, Ray P, Ray A. Treg-mediated immunosuppression involves activation of the Notch-HES1 axis by membrane-bound TGF-beta. J Clin Invest. 2006; 116:996–1004. [PubMed: 16543950]
26. Chen CY, Huang D, Wang RC, Shen L, Zeng G, Yao S, Shen Y, Halliday L, Fortman J, McAllister M, et al. A critical role for CD8 T cells in a nonhuman primate model of tuberculosis. PLoS Pathog. 2009; 5:e1000392. [PubMed: 19381260]
27. Shen Y, Zhou D, Qiu L, Lai X, Simon M, Shen L, Kou Z, Wang Q, Jiang L, Estep J, et al. Adaptive immune response of Vgamma2Vdelta2+ T cells during mycobacterial infections. Science. 2002; 295:2255–2258. [PubMed: 11910108]
28. Wei H, Huang D, Lai X, Chen M, Zhong W, Wang R, Chen ZW. Definition of APC presentation of phosphoantigen (E)-4-hydroxy-3-methyl-but-2-enyl pyrophosphate to Vgamma2Vdelta 2 TCR. J Immunol. 2008; 181:4798–4806. [PubMed: 18802083]
29. Wei H, Wang R, Yuan Z, Chen CY, Huang D, Halliday L, Zhong W, Zeng G, Shen Y, Shen L, et al. DR*W201/P65 tetramer visualization of epitope-specific CD4 T-cell during M. tuberculosis infection and its resting memory pool after BCG vaccination. PLoS One. 2009; 4:e6905. [PubMed: 19730727]
30. Zeng G, Chen J, Zhong L, Wang R, Jiang L, Cai J, Yan L, Huang D, Chen CY, Chen ZW. NSOM- and AFM-based nanotechnology elucidates nano-structural and atomic-force features of a Y. pestis V immunogen-containing particle vaccine capable of eliciting robust response. Proteomics. 2009; 9:1538–1547. [PubMed: 19253301]
31. Chen Y, Qin J, Chen ZW. Fluorescence-topographic NSOM directly visualizes peak-valley polarities of GM1/GM3 rafts in cell membrane fluctuations. J Lipid Res. 2008; 49:2268–2275. [PubMed: 18603643]
32. Chen Y, Shao L, Ali Z, Cai J, Chen ZW. NSOM/QD-based nanoscale immunofluorescence imaging of antigen-specific T-cell receptor responses during an in vivo clonal V{gamma}2V{delta}2 T-cell expansion. Blood. 2008; 111:4220–4232. [PubMed: 18039956]
33. Yong Chen JQ, Cai Jiye, Chen Zheng W. Cold Induces Micro/nano-scale Reorganization of Lipid Raft Markers at Mounds of Cell-membrane Fluctuations. Plos One. 2009
34. Huang D, Shen Y, Qiu L, Chen CY, Shen L, Estep J, Hunt R, Vasconcelos D, Du G, Aye P, et al. Immune distribution and localization of phosphoantigen-specific Vgamma2Vdelta2 T cells in lymphoid and nonlymphoid tissues in Mycobacterium tuberculosis infection. Infect Immun. 2008; 76:426–436. [PubMed: 17923514]
35. Gong G, Shao L, Wang Y, Chen CY, Huang D, Yao S, Zhan X, Sicard H, Wang R, Chen ZW. Phosphoantigen-activated V gamma 2V delta 2 T cells antagonize IL-2-induced CD4+CD25+Foxp3+ T regulatory cells in mycobacterial infection. Blood. 2009; 113:837–845. [PubMed: 18981295]
36. Dumoutier L, Lejeune D, Colau D, Renauld JC. Cloning and characterization of IL-22 binding protein, a natural antagonist of IL-10-related T cell-derived inducible factor/IL-22. J Immunol. 2001; 166:7090–7095. [PubMed: 11390453]
37. Yao S, Huang D, Chen CY, Halliday L, Zeng G, Wang RC, Chen ZW. Differentiation, distribution and gammadelta T cell-driven regulation of IL-22-producing T cells in tuberculosis. PLoS Pathog. 2010; 6:e1000789. [PubMed: 20195465]

38. Fooksman DR, Vardhana S, Vasiliver-Shamis G, Liese J, Blair D, Waite J, Sacristan C, Victora G, Zanin-Zhorov A, Dustin ML. Functional Anatomy of T Cell Activation and Synapse Formation. Annu Rev Immunol. 2009

39. Zhong L, Zeng G, Lu X, Wang RC, Gong G, Yan L, Huang D, Chen ZW. NSOM/QD-based direct visualization of CD3-induced and CD28-enhanced nanospatial coclustering of TCR and coreceptor in nanodomains in T cell activation. PLoS One. 2009; 4:e5945. [PubMed: 19536289]

40. Dumoutier L, Louahed J, Renauld JC. Cloning and characterization of IL-10-related T cell-derived inducible factor (IL-TIF), a novel cytokine structurally related to IL-10 and inducible by IL-9. J Immunol. 2000; 164:1814–1819. [PubMed: 10657629]

41. Dhiman R, Indramohan M, Barnes PF, Nayak RC, Paidipally P, Rao LV, Vankayalapati R. IL-22 produced by human NK cells inhibits growth of Mycobacterium tuberculosis by enhancing phagolysosomal fusion. J Immunol. 2009; 183:6639–6645. [PubMed: 19864591]

42. Canaday DH, Wilkinson RJ, Li Q, Harding CV, Silver RF, Boom WH. CD4(+) and CD8(+) T cells kill intracellular Mycobacterium tuberculosis by a perforin and Fas/Fas ligand-independent mechanism. J Immunol. 2001; 167:2734–2742. [PubMed: 11509617]

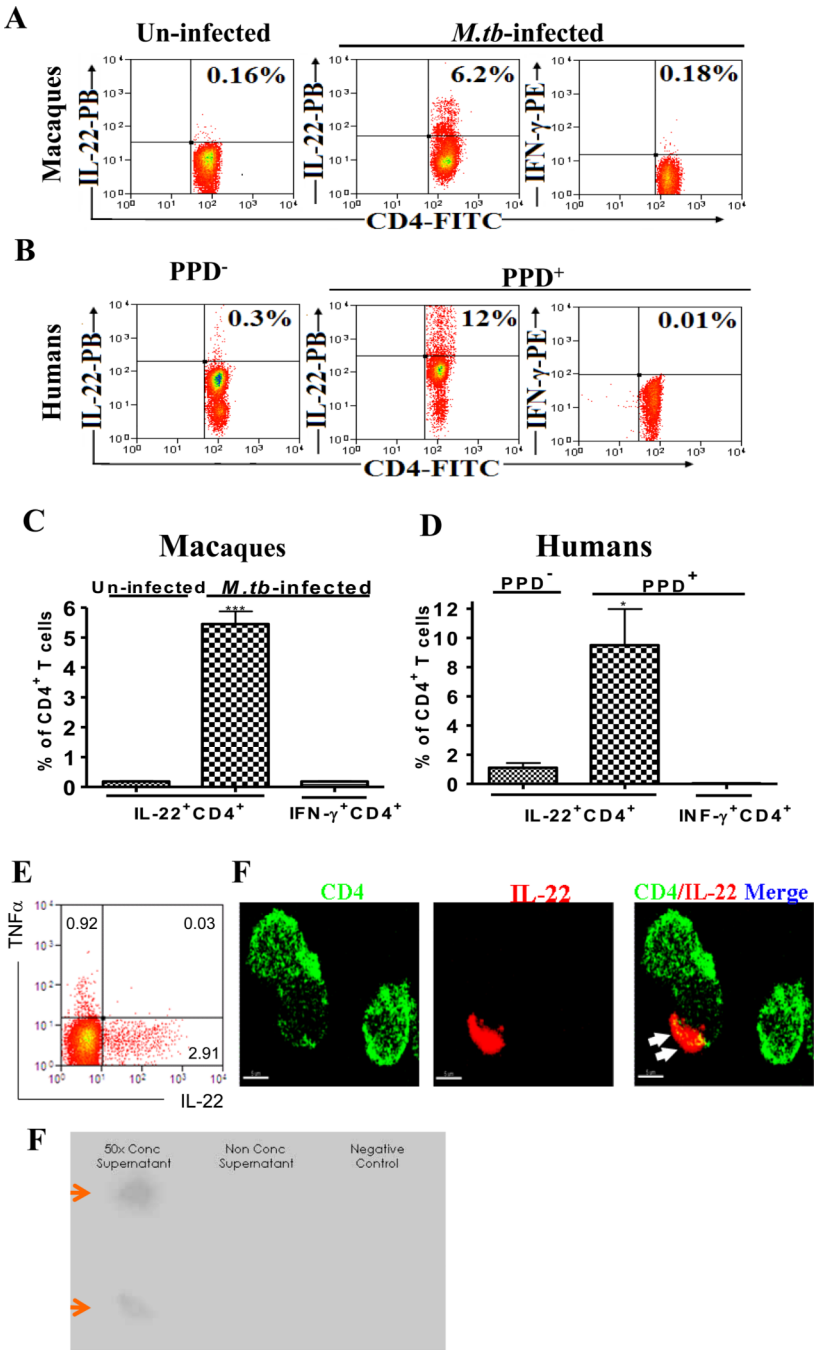

Fig.1. Upon activation, CD4+ T cells in *M. tuberculosis*-infected macaques and humans differentiated into T effector cells bearing membrane-bound IL-22 after *de novo* IL-22 production

Percentage numbers of CD4+ T cells bearing membrane-bound IL-22 or CD4+ T cells expressing membrane-bound-IFN-γ are shown in the upper right quadruple of flow cytometry histograms. Data were gated on CD4 T cells. All cells were surface-stained directly without treatment with membrane permeabilization reagents. No membrane-bound IL-22 were detected for negative controls (see the Methods section). Membrane-bound IL-22 did not appear to be specific for *M. tuberculosis* infection as CD4+ T cells from

listeria-vaccinated macaques could also express membrane-bound IL-22 upon activation by CD3/CD28 Ab (data not shown).

Fig.1A. Representative flow cytometry histograms show that *M. tuberculosis* stimulation of PBMC from *M. tuberculosis*-infected macaques induced membrane-bound IL-22+ CD4+ T effector cells, whereas CD4+ T cells in PBMC from un-infected macaques contained very few membrane-bound IL-22+ T effectors. PBMC from infected macaques were isolated from the blood collected two months after *M. tuberculosis* infection. Only 0.18% of CD4+ T cells expressing membrane-bound IFN-γ was detectable in *M. tuberculosis*–infected PBMC. PBMC of macaques were infected with *M. tuberculosis* in 96-well plates in MOI=1 for 18 hours prior to analysis.

Fig.1B. Representative flow cytometry histograms show that *M. tuberculosis* stimulation of PBMC from PPD^+ human donors induced 12% of CD4+ T cells bearing membrane-bound IL-22. Only ~0.3% of CD4 T cells bearing membrane-bound IL-22 were detected in PBMC isolated from PPD^- donors. Also, only ~0.01% of CD4 T cells expressing membrane-bound-IFN-γ could be detected in blood lymphocytes of PPD^+ donors. Human PBMC were similarly infected with *M. tuberculosis* as described above or stimulated overnight with anti-CD3/anti-CD28 in presence of PPD and stained without cell permeabilization treatment.

Fig.1C. Bar graphics data shows that *M. tuberculosis*-infected macaques exhibited significantly greater numbers of CD4+ T cells bearing membrane-bound IL-22 than un-infected macaques after *M. tuberculosis* stimulation *in vitro* (*** $p<0.001$, n=3). Data are mean percentage numbers among CD4+ T cells with error bars of SEM derived from three rhesus macaques.

Fig.1D. Bar graphic data shows that PPD^+ human donors exhibited significantly greater numbers of CD4+ T cells bearing membrane-bound IL-22 than PPD^- donors after *M. tuberculosis* stimulation *in vitro* (* $p<0.05$, n=3). Data are mean percentage numbers among CD4+ T cells with error bars of SEM derived from three different donors.

Fig.1E. A representative flow cytometry data showing that IL-22-producing CD4+ T cells do not co-express TFN-α(CD4-gated). No co-expression of IFN-γ was found either (data not shown). Cells were isolated from peripheral blood of *M. tuberculosis*-infected macaques. Similar data were observed in five different macaques.

Fig. 1F. A representative confocal microscopic image shows that IL-22 forms the capping domain (as marked by white arrow heads) and co-localizes in part with CD4 on T-cell membrane. Cells were isolated from the blood of *M. tuberculosis*-infected macaques, and were stained directly with anti-IL-22 and anti-CD4 antibodies without membrane permeabilization reagents.

Fig.1G. IL-22 in concentrated culture supernatant (left panel) from activated, enriched CD4+ T cells could be detected by the dot-blot assay. CD4+ T cells from spleens of *M. tuberculosis*-infected macaques (ID 7713, 7714) were enriched by deleting CD8+ cells using immune-magnetic beads as described above. ~1×10^7 enriched CD4+ T cells were stimulated by PPD in culture for two days. Supernatants were collected, either un-concentrated or concentrated 50× using Vivacell concentrator(Vivasciences)(28, 29), and then tested for IL-22 by the dot plot assay as we described (28, 29). Negative control(right) was culture supernatant from un-stimulated PBL of uninfected macaques. We used the dot blot assay as ELISA assay for quantitation of macaque IL-22 was not commercially available.

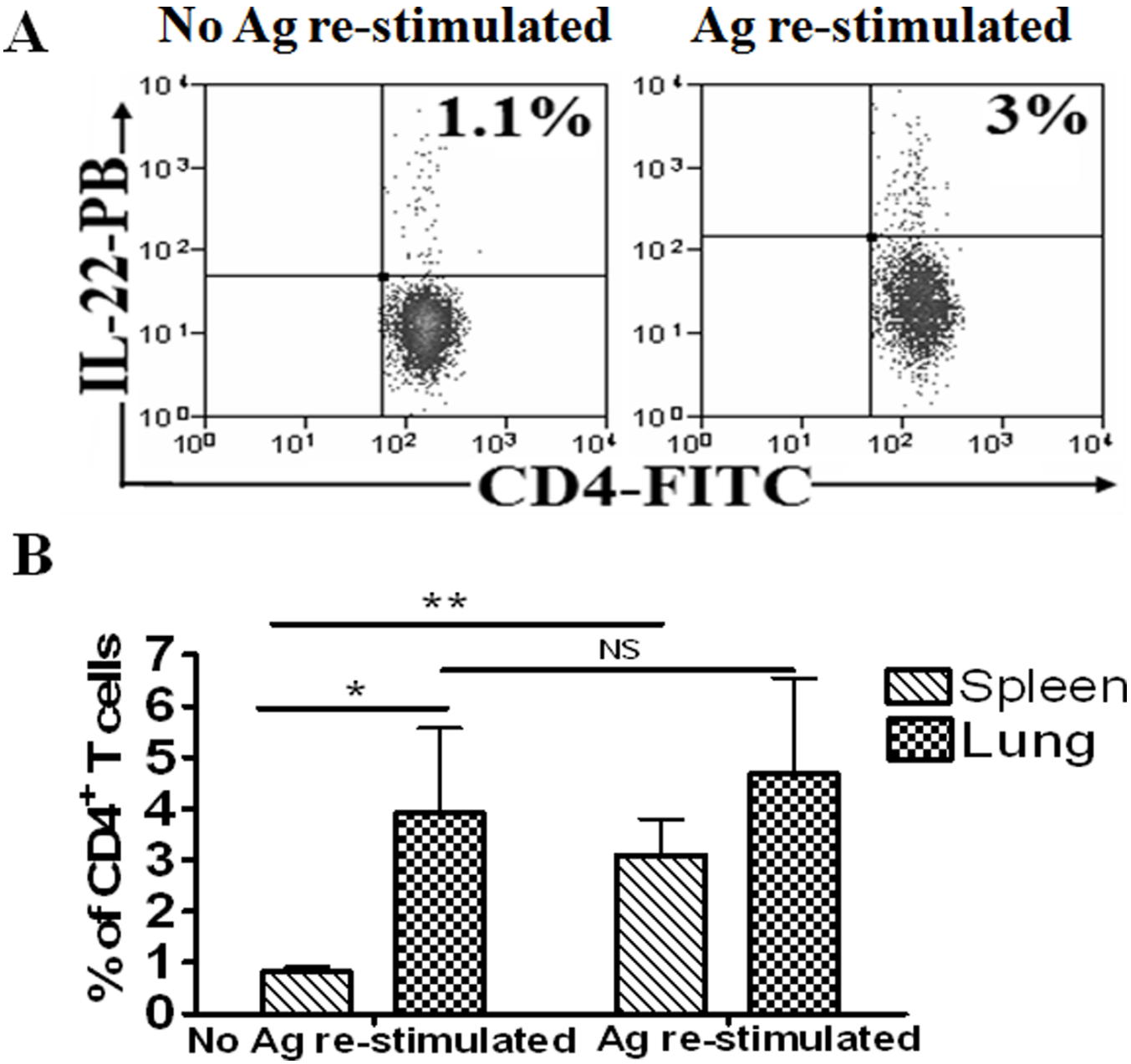

Fig.2. Membrane-bound IL-22+ CD4+ T cells matured *in vivo* and sustained in highly inflammatory environments during active *M. tuberculosis* infection

All cells used for experiments were not treated with cell permeabilization reagents during staining. For experiments without *in vitro* Ag re-stimulation, lymphocytes isolated from the spleens or lungs of *M. tuberculosis*–infected macaques (two months after infection) were stained directly with anti-IL-22 Abs conjugating fluorochromes. Matched normal serum or isotype control Ab did not confer detectable staining of IL-22 as analyzed by flow cytometry (data not shown). Also, control PBMC from SHIV-infected macaques displayed undetectable staining of membrane-bound IL-22+ CD4+ T cells (data not shown). Data were gated on CD4+ T cells.

Fig.2A. Left panel: A representative flow cytometry histogram showing that 1.1% of CD4+ T cells expressing membrane-bound IL-22 could be directly detected without any *in vitro*

Ag stimulation in lymphocytes isolated from the spleens of *M. tuberculosis*-infected macaques. **Right panel**: A representative flow cytometry histogram showing that, after *in vitro* Ag stimulation, 3.0% of CD4+ T cells expressing membrane-bound-IL-22 could be detected in lymphocytes isolated from the spleens of *M. tuberculosis*-infected macaques. Percentage numbers of membrane-bound IL-22+ CD4+ T cells are shown in the upper right quadruple of flow cytometry histograms. For *in vitro* Ag stimulation, lymphocytes isolated from spleens or lungs were stimulated with pooled ESAT-6 and Ag85B peptides in the presence of CD28/CD49d, and then stained directly with Abs without membrane permeabilization.

Fig.2B. Bar graphic data shows that lymphocytes from the lung tissues contained much higher percentages of membrane-bound IL-22+CD4+ T cells than those from the spleens when surface-stained without Ag stimulation(*$p<0.05$). After Ag stimulation, no significant increases (NS) in membrane-bound IL-22+CD4+ T cells were detected in lung lymphocytes, although increases in these effector cells could be seen in spleen lymphocytes after *in vitro* Ag stimulation (**$p<0.01$.). Data are mean percentage numbers among CD4+ T cells with error bars of SEM derived from four rhesus macaques. In general, <2% of un-stimulated CD4+ T cells in the blood from *M. tuberculosis*-infected macaques expressed membrane-bound IL-22. The studied macaques had ~1000 CFU/10 ml lung tissue lysate but had no or very few CFU measurable in the spleen tissue lysate. Also, these macaques showed severe TB lesions only in lung tissues but mostly no gross lesions in the spleen tissues.

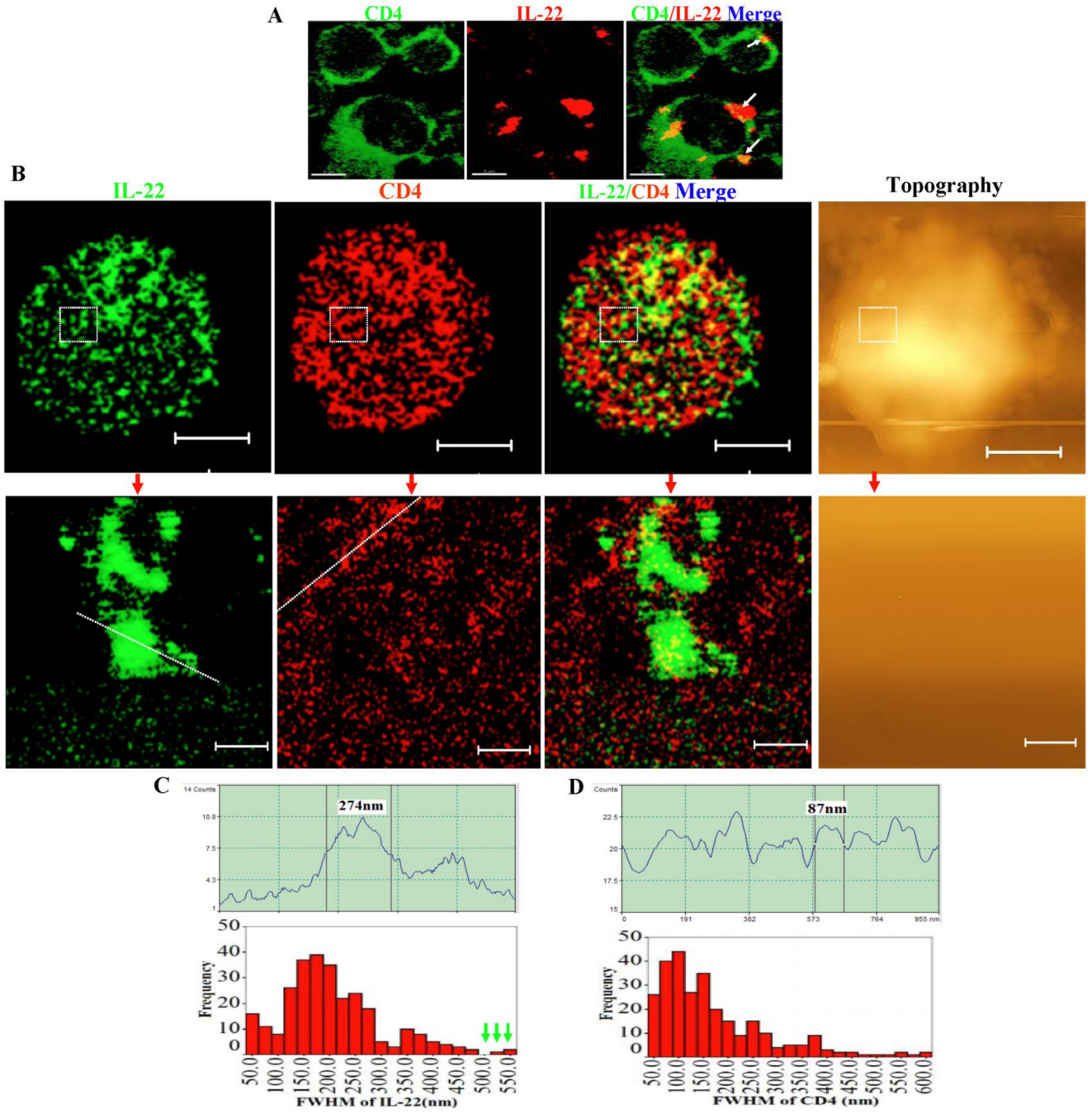

Fig.3. Membrane-bound IL-22 molecules were engaged as ~100–200 nm nanoclusters or ~300–600 nm high-density nanodomains on membrane of IL-22+CD4+ T effectors

No membrane-bound IL-22 were detected for negative controls (see the Methods section). **Fig.3A. Confocal microscopic images show that membrane-bound IL-22 formed capping domains on CD4 T cells after *in vivo M. tuberculosis* infection.** Lymphocytes isolated from the spleens of *M. tuberculosis*-infected macaques (two months after infection) were surface-stained with anti-IL-22 Ab, without *in vitro* Ag stimulation or membrane permeabilization. This only allowed membrane-bound IL-22 to be stained and visualized by confocal microscopy. The white arrow heads indicated “membrane-bound” IL-22 on CD4+ T cells. Note that membrane-bound IL-22 forms capping domains on CD4+ T cell surface.

No membrane-bound IL-22 was observed in PBMC from un-infected macaques (data not shown). Isotype control IgG did not stain cell membrane of PBMC from infected macaques (data not shown).

Fig.3B. Representative NSOM/QD-based nanoscale imaging shows that membrane-bound IL-22 are engaged as ~100–200 nm nanoclusters or as ~300–600 nm high-density nanodomains. Upper panels show fluorescence imaging of two-color molecular staining of IL-22(green) and CD4(red) on outer membrane and representative topography (right) for one representative membrane-bound IL-22+CD4+ T effector cell. Note that NSOM/QD-based nanoscale imaging only detects fluorescence dots on outer membrane but not underneath (see text). Few IL-22 molecules co-localize with CD4 in the merged image. Lower panels show the enlarged images derived from re-scanning the dashed squares in the IL-22 and CD4 images and topography in the upper panels. The scale bars for upper and lower panels are 3.214 μm and 385 nm, respectively. The staining samples for NSOM/QD imaging were similarly prepared as those for confocal imaging. Integration time for all the images is 30 ms with 400×400 scanning lines.

Fig.3C. Upper panel: A representative fluorescent intensity profile of an IL-22 nanocluster. The fluorescent intensity profile (upper) of the cross section of the objects is marked by a line in the fluorescence image. Shown is an IL-22 nanocluster with diameters of 274 nm (FWHM). **Lower panel**: histogram graph shows the frequency of different sizes of FWHM of IL-22 nanoclusters on the CD4+ T cells. The green arrow heads marked the FWHM of IL-22 microdomains (>500 nm).

Fig.3D. Upper panel: A representative fluorescence intensity profile of a CD4 nanocluster. The fluorescent intensity profile (Upper) of the cross section of the objects is marked by a line in the fluorescence image as well. Shown are a CD4 clusters with diameters of 87 nm (FWHM). **Lower panel**: histogram graph shows the frequency of different sizes of FWHM of CD4 nanoclusters or nanodomains on the CD4+ T cells.

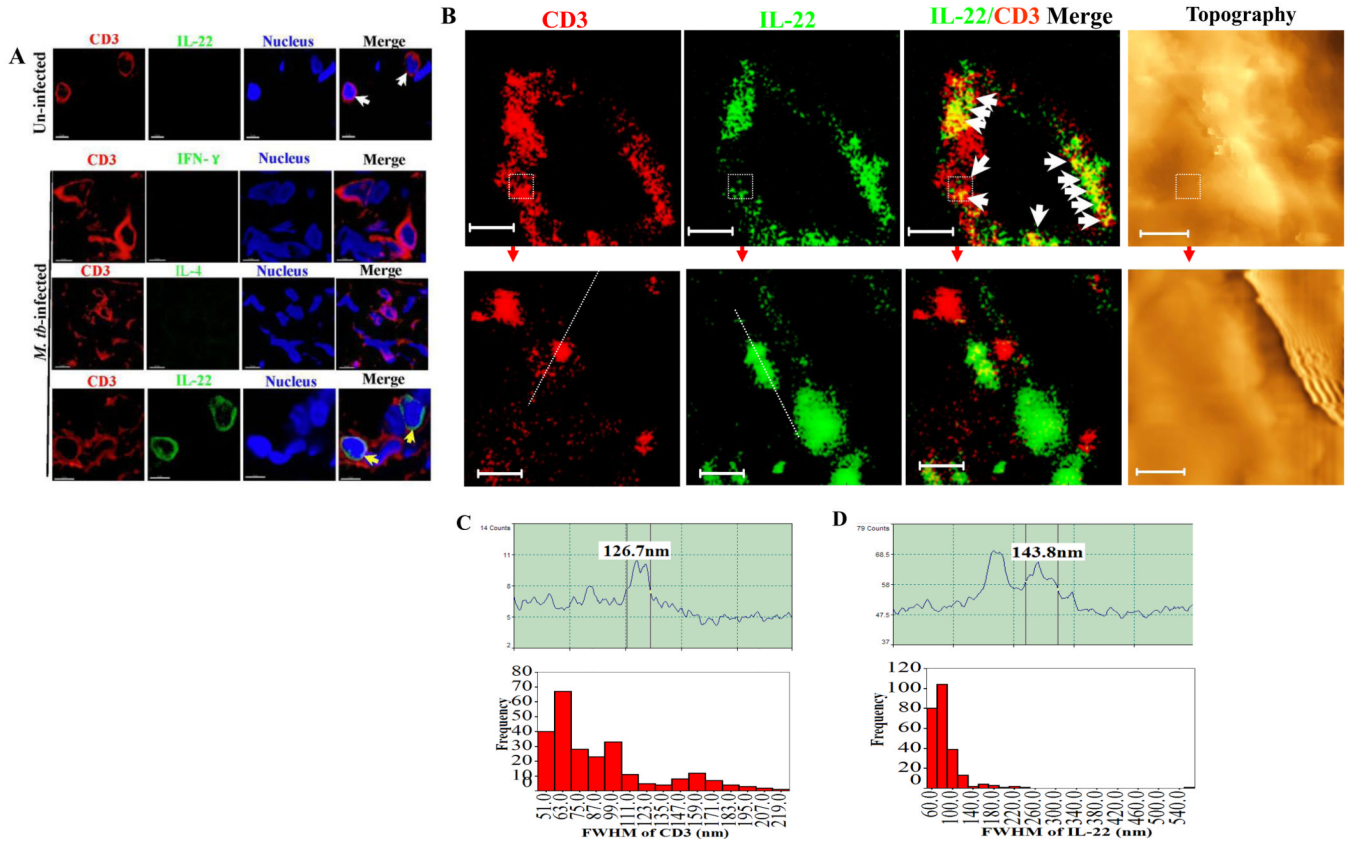

Fig.4. Membrane-bound IL-22 distributed within membrane sharing similar distribution with membrane CD3 molecules of T cells in TB lung tissue sections

Fig.4A. Representative *in situ* confocal microscopic images (63× NA) in the bottom panel show that IL-22 appeared to co-localize with CD3 (marked by yellow arrows) in the membrane of $CD3^+$ T cells in lung tissue sections prepared from the right middle lung lobe containing granulomas. The images at the top panel show that no IL-22 (white arrows) was detectable in control CD3 T cells in the peri-bronchiolar lymphoid lung section derived from one of three un-infected, healthy macaques. No INF-γ or IL-4 was detectable in the T-cell membrane from the same lung TB tissue sections. Matched normal serum or control isotype IgG did not give rise to any membrane IL-22 staining in the lung TB tissue sections (data not shown).

Fig.4B. Representative *in situ* NSOM/QD-based nanoscale imaging of membrane-bound IL-22 distributed within membrane sharing similar distribution with membrane CD3 molecules of T cells in TB lung tissue sections. Upper panels show *in situ* fluorescence imaging of two-color molecular staining of CD3(red) and IL-22(green) and topography for one representative IL-22+CD3+ T cell in the lung tissue section. White arrow heads in IL-22/CD3 merge images indicate that IL-22 and CD3 similarly localized in the cell membrane rather than in the cytoplasm. Lower panels show the enlarged images derived from re-scanning the dashed squares in the CD3, IL-22, merge images and topography, respectively, in the upper panels. Scale bars for the upper and lower panels are 2.9 μm and 391 nm, respectively. Similar NSOM images were seen from five IL-22+CD3+ T cells in the lung tissue sections.

Fig.4C. Upper panel: A representative fluorescence intensity profile of a CD3 nanocluster. The fluorescent intensity profile (upper) of the cross section of the objects is marked by a line in the fluorescence image as well. Shown is a CD3 cluster with diameters of 126 nm

(FWHM). Lower panel: histogram graph shows the frequency of different sizes of FWHM of CD3 nanoclusters or nanodomains on the CD3+ T cells.

Fig.4D. Upper panel: A representative fluorescent intensity profile of an IL-22 nanocluster. The fluorescent intensity profile (upper) of the cross section of the objects is marked by a line in the fluorescence image. Shown is an IL-22 cluster with diameters of 143 nm (FWHM). Lower panel: histogram graph shows the frequency of different sizes of FWHM of IL-22 nanoclusters on CD3+ T cells.

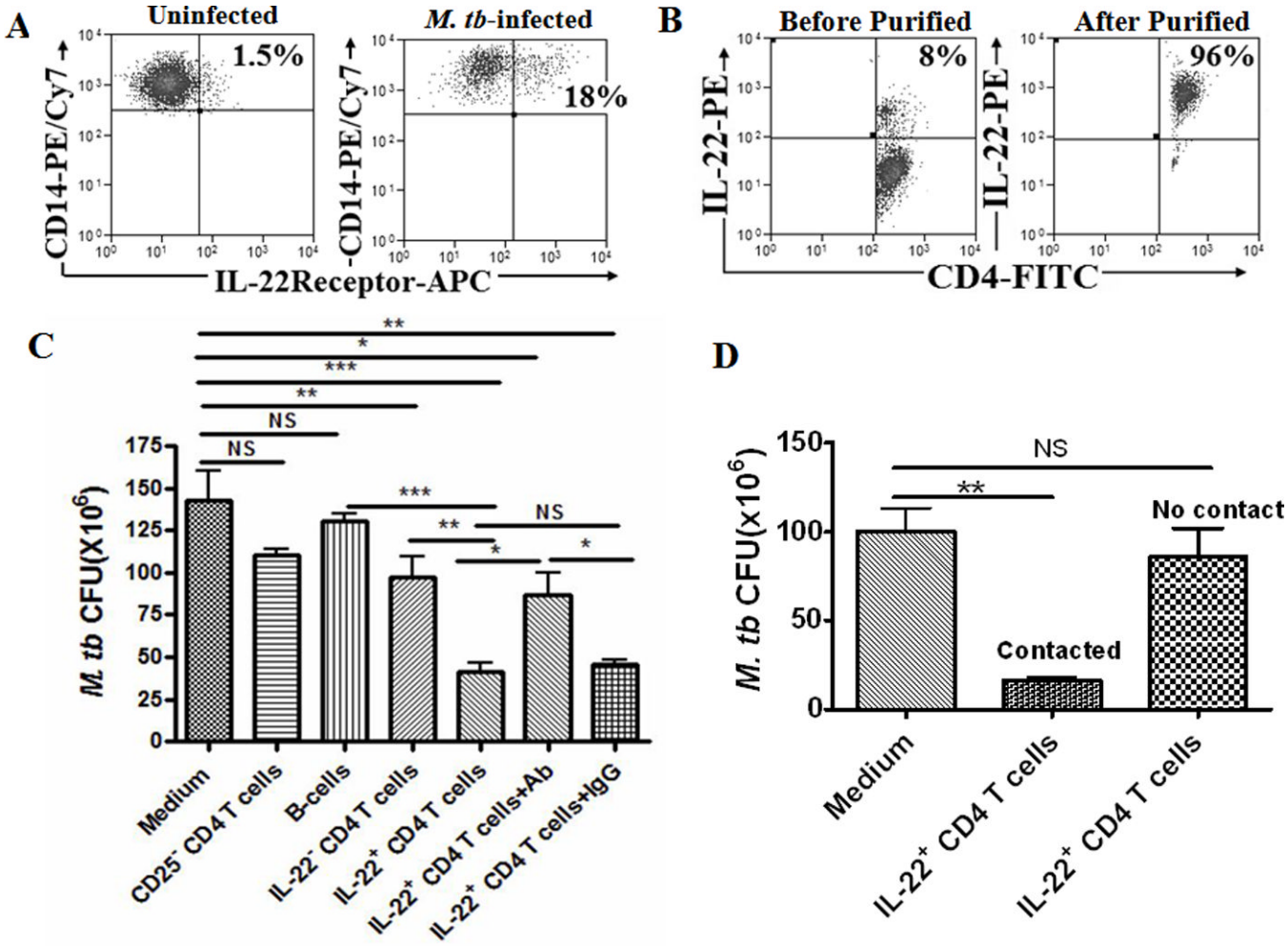

Fig.5. Membrane-bound IL-22$^+$CD4$^+$ T cells inhibited intracellular *M. tuberculosis* replication in monocyte-derived macrophages

Fig.5A. Flow cytometry characterization of IL-22R expression induced by *M. tuberculosis* infection of macrophages. Monocytes-derived macrophages were stained with IL-22R and CD14, and analyzed by flow cytometry. Left panel: A representative flow cytometry histogram shows that only 1.5% of IL-22R-expressing CD14$^+$ macrophages (gated on CD14) were observed in monocytes-derived macrophages without *M. tuberculosis* infection. Right panel: A representative flow cytometry histogram shows that after *in vitro M. tuberculosis* infection, about 18% of CD14$^+$ macrophages (gated on CD14) expressed IL-22R(upper right quadruple). Similar results were seen in other five independent experiments.

Fig.5B. Representative flow cytometry data show that immunomagnetic beads-based purification could enrich IL-22+CD4+ T cells to the level of 70–96%. Similar results were observed in six other repeated experiments.

Fig.5C. Bar graphic data shows that IL-22+ CD4+ T cells inhibited intracellular *M. tuberculosis* replication in monocyte-derived macrophages. *M. tuberculosis*-infected macrophages (5×10^4) were co-cultured with medium alone, CD20$^+$ B cells(5×10^5), CD25$^-$CD4$^+$ T cells(5×10^5), IL-22$^-$CD4$^+$ T cells (5×10^5), IL-22+CD4+ T cells (5×10^5), or IL-22$^+$CD4$^+$ T cells (5×10^5)+anti-IL-22 Ab(10μg/ml), IL-22+CD4+ T cells (5×10^5)+IgG(10μg/ml) for 4 days. The cultured cells were lysed and CFU counts in lysate were determined as described in the Methods section. Enriched IL-22+CD4+ T cells (5×10^5)

significantly reduced *M. tuberculosis* CFU counts when compared with control cultures (***p<0.001, ***p<0.001, **p<0.01, respectively). Blocking of membrane-bound IL-22 by anti-IL-22 Ab but not isotype IgG control from the beginning throughout the assay led to a reduced capability of IL-22+CD4 T cells to inhibit intracellular *M. tuberculosis* (*p<0.05, NS, no significant difference). Data were mean values with error bars of SEM derived from four rhesus macaques in five independent experiments. The marked reduction in CFU counts were interpreted as "inhibition" in the text, although "killing" was implicative based on the growth kinetics of *M. tuberculosis* on day 0, 2, 4 after infection (data not shown).
Fig.5D. Bar graphic data shows that *M. tuberculosis* growth in monocyte-derived macrophages was inhibited by contact IL-22+CD4+ T cells (contacting with infected macrophages), but not those non-contact IL-22+CD4+T cells or culture medium containing IL-22 secreted by the IL-22+CD4+ T effector cells. *M. tuberculosis-infected* macrophages (5×10^4) were co-cultured in Transwell system with medium alone, contact IL-22+CD4+ T cells (5×10^5), non-contact IL-22+CD4+ T cells (5×10^5) for 4 days prior to bacteria counts. Non-contact means that enriched IL-22+CD4+ T cells were placed in the upper chamber of Transwell culture system without "physical" contact with infected macrophages that were cultured in the lower chamber. Therefore, non-contact IL-22+CD4+ T cells did not contact macrophages but secretory IL-22 in the medium could trans-pass through the micro-holes and reach macrophages in the lower chamber. Secretory IL-22 was detectable in the concentrated culture medium. Contact means that IL-22+CD4+ T cells and infected macrophages were co-cultured in the lower chamber of Transwell culture system. Data in graph were mean values with error bars of SEM derived from four rhesus macaques. **p<0.01, NS, no significant difference.